Radiological Physics and Technology (2019) 12:118–125
https://doi.org/10.1007/s12194-019-00498-7

The use of combined T_2-weighted and FLAIR synthetic magnetic resonance images to improve white matter region contrast: a feasibility study

Yasuhiro Fujiwara[1] · Yumi Inoue[2] · Masayuki Kanamoto[3] · Shota Ishida[3] · Toshiki Adachi[3] · Hirohiko Kimura[4]

Received: 12 June 2018 / Revised: 9 January 2019 / Accepted: 11 January 2019 / Published online: 21 January 2019

Abstract
Synthetic magnetic resonance imaging (MRI) allows the production of images with any contrast from a single scan after quantification. The combined T_2-weighted image (T2WI) and fluid-attenuated inversion recovery (FLAIR) image is expected to have an improved contrast between the normal-appearing white matter (WM) and WM lesion (WML). The purpose of this study was to determine whether optimal T_2 contrast-weighted images (SyFLAIR^3) comprising the combined T2WI and FLAIR image generated using synthetic MRI could improve contrast in the WM region. Numerical simulations were performed to estimate the contrast-to-noise ratio (CNR) between the WM and WML and cerebrospinal fluid (CSF) ratio at any echo time (TE) using SyFLAIR^3. The CNR and CSF ratio for SyFLAIR^3 was compared with those for FLAIR and double inversion recovery (DIR) images in ten volunteers. In numerical simulations, the CNR for SyFLAIR^3 was increased in the T2WI and FLAIR images with long TEs, and the CSF ratio was decreased on those with short TEs. An in vivo study indicated that the CNR for SyFLAIR^3 using T2WI and FLAIR images with an optimized combination of TEs was significantly higher than those for FLAIR and DIR images; whereas, the CSF ratio for the optimized SyFLAIR^3 was not significantly different from that for the FLAIR images. The use of SyFLAIR^3 improves the contrast within the region of the WM without the need for additional scanning in synthetic MRI.

Keywords Magnetic resonance imaging (MRI) · Synthetic MRI · Quantitative MRI · White matter lesion · Multiple sclerosis

1 Introduction

Multiple sclerosis (MS) is a disease of the central nervous system, which is characterized by infiltration of inflammatory cells and demyelination around the regions of normal-appearing white matter (WM). A magnetic resonance imaging (MRI) finding as a primary biomarker is important in the diagnosis of MS [1, 2]. Detection of MS lesions using MRI has been used for the purpose of evaluation of treatment efficacy and follow-up during the focal stage of the disease. Detection of the MS lesion at an early stage is important to estimate the risks of future relapse, disability, and cognitive deficits [1, 3].

MS lesions show prolonged T_2 relaxation time and higher signal intensity than the peripheral tissue on T_2-weighted images (T2WIs) and fluid-attenuated inversion recovery (FLAIR) images [4–7]. To improve the accuracy of MS diagnosis, higher T_2 contrast in the WM region with concomitant suppression of signal intensity of the cerebrospinal fluid (CSF) is necessary. Several imaging techniques to improve the contrast of the MS lesion have been reported, such as phase-sensitive inversion recovery (PSIR) and double inversion recovery (DIR) sequences [8–12].

Synthetic MRI is a technique to quantify the T_1 value, T_2 value, and proton density (PD) with simultaneous correction of the B_1 homogeneity using a single pulse sequence [13].

✉ Yasuhiro Fujiwara
yfuji@kumamoto-u.ac.jp

1 Department of Medical Imaging, Faculty of Life Sciences, Kumamoto University, 4-24-1 Kuhonji, Chuo-ku, Kumamoto 862-0976, Japan

2 Course of Radiological Science, School of Health Sciences, Kumamoto University, Kumamoto, Japan

3 Radiological Center, University of Fukui Hospital, Fukui, Japan

4 Department of Radiology, University of Fukui, Fukui, Japan

After acquisition of the imaging data and quantification of the T_1 value, T_2 value, and PD, the images can be generated with any contrast weighting by freely adjusting parameters such as the repetition time (TR), echo time (TE), and inversion time (TI) without the need for additional scanning [9, 14]. Recent reports indicated that FLAIR, DIR, and PSIR images generated using synthetic MRI improved the contrast of MS plaque and WM lesions (WMLs) [9, 15]. Thus, it is possible to improve the lesions' detectability for specific diseases by generating characteristic contrast-weighted images from synthetic MRI.

Techniques involving combinations of images are effective to improve the detection of WMLs [16–18]. Gabr et al. reported that post-acquisition combination images generated from three-dimensional (3D) T2WI and FLAIR images ($FLAIR_3$) improved the visualization of WMLs [18]. $FLAIR_3$ images are generated by multiplying the signal intensity of T2WI and FLAIR images after raising the T2WI and FLAIR image to an arbitrary power to maximize the contrast-to-noise ratio (CNR) between the WM and WMLs. The proposed approach is easy to use in a clinical setting because sophisticated pulse sequence modifications are not required for acquisition of the $FLAIR_3$ image; however, the acquisition process for each 3D image is time-consuming, which may result in motion artifacts or displacements between two successive image acquisitions.

In this study, we produced synthetic $FLAIR_3$ images ($SyFLAIR^3$) from T2WIs and FLAIR images with optimal contrast weighting using synthetic MRI. We hypothesized that the combined T2WI and FLAIR image generated by synthetic MRI would improve the lesions' contrast in the WM region. The study aimed to determine the optimal contrast weighting for $SyFLAIR^3$ and evaluate the benefits of improving T_2 contrast in the WM region.

2 Materials and methods

2.1 Production of SyFLAIR^3

To adjust the image contrast, γ-correction is applied by raising the signal intensity to the positive γ power: increasing γ to >1 improves the contrast of the region with high signal intensity; however, the contrast of the region with intermediate-level signals decreases conversely as γ increases. In this study, we attempted to raise the signal intensities of the two images to the γ power of different values and multiplied the obtained images. The sum of applied γ values should be <3 to achieve improved contrast of the lesion with high signal intensity, while maintaining the contrast of the intermediate-level signals at 80% [18]. Thus, the images produced by multiplying the FLAIR images by T2WIs with γ-correction at the specified range are expected to increase contrast of the WMLs, such as those in patients with MS, and suppress the CSF signal.

Imaging using the DIR sequence is a direct approach to obtain a contrast-enhanced image of the WML. Although the DIR image achieves higher contrast between the WML and WM, the SNR of the image is lower than those of the T2WI and FLAIR image because of its low signal intensity; hence, lesions with small size and low contrast on a DIR image may be obscured by noise and remain undetected. In contrast, in case of available T2WIs and FLAIR images, the $FLAIR_3$ image may obtain a higher CNR compared with that of the DIR image, resulting in a higher SNR and contrast of the WML and WM. In addition, the advantages of applying this principle to synthetic MRI are that it is easy to implement and the combined images can be produced from images generated at optimal parameters and arbitrary TR/TE settings without normalizing or matching the signal intensity.

Signal intensity for $SyFLAIR^3$ was calculated using a general multiplicative combination of the T2WI and FLAIR image, as shown in the following equation:

$$S_{\mathrm{SyFLAIR3}} = S_{\mathrm{T2WI}}^{\alpha} \cdot S_{\mathrm{FLAIR}}^{\beta}, \tag{1}$$

where S_{T2WI} and S_{FLAIR} represent the signal intensities of the T2WI and FLAIR image obtained using the synthetic MRI sequence, respectively; α and β are positive exponents with optimized values of 1.45 and 1.55, respectively, as previously reported [18].

2.2 Numerical simulations

Signal intensities of the WM, WMLs, gray matter (GM), CSF, and noise on $SyFLAIR^3$ were calculated using TE values in the range of 20–140 ms at 20-ms intervals for the T2WI and FLAIR image. Signal intensity of the T2WI and FLAIR image was estimated as follows [14]:

$$S_{\mathrm{T2WI}} = k \cdot \mathrm{PD} \cdot \left(1 - \mathrm{e}^{-\mathrm{TR}/T_1}\right) \cdot \mathrm{e}^{-\mathrm{TE}/T_2}, \tag{2}$$

$$S_{\mathrm{FLAIR}} = k \cdot \mathrm{PD} \cdot \left(1 - 2 \cdot \mathrm{e}^{-\mathrm{TI}/T_1} + \mathrm{e}^{-\mathrm{TR}/T_1}\right) \cdot \mathrm{e}^{-\mathrm{TE}/T_2}, \tag{3}$$

where S_{T2WI} and S_{FLAIR} represent the signal intensity of the T2WI and FLAIR image, respectively; k is a scaling factor. TR, TE, and TI represent the repetition time, echo time, and inversion time, respectively. PD, T_1, and T_2 represent the proton density, T_1 value, and T_2 value for each tissue, respectively. Parameters used in the calculation for each tissue are shown in Table 1 [18]. The T_1 value, T_2 value, and PD of

Table 1 The parameters used for the calculation of the signal intensity for each tissue

Tissue	T_1 value (ms)	T_2 value (ms)	Proton density
White matter	850	85	0.71
Gray matter	1400	100	0.83
Cerebrospinal fluid	4000	2000	1
White matter lesion	978	98	1.83

the WMLs were assumed to be prolonged by 15% compared with those of the WM [18].

Numerical simulation was performed to estimate the CNR of the WM region and CSF ratio for SyFLAIR^3 at each combination of TEs for the T2WI and FLAIR image. The CNR of the WM and WMLs for SyFLAIR^3 was calculated for each TE combination as follows:

$$\mathrm{CNR} = \frac{S_{\mathrm{WML}} - S_{\mathrm{WM}}}{N_{\mathrm{SyFLAIR3}}}, \tag{4}$$

where S_{WML}, S_{WM}, and N_{SyFLAIR3} represent the signal intensity of the WML, WM, and noise for SyFLAIR^3, respectively. To estimate the CNR for SyFLAIR^3, the simulated noise of the T2WI and FLAIR image was defined as the root mean square of the WM signal intensity for images generated at each TE. The levels of the simulated signal intensity of the T2WI and FLAIR image are not matched and hence, their image noise is also different. The noise for SyFLAIR^3 (N_{SyFLAIR3}) was defined as the standard deviation of the simulated signal intensity for SyFLAIR^3 based on the law of error propagation and estimated using the following equation:

$$\left(\frac{N_{\mathrm{SyFLAIR3}}}{S_{\mathrm{SyFLAIR3}}}\right)^2 = \alpha^2\left(\frac{N_{\mathrm{T2WI}}}{S_{\mathrm{T2WI}}}\right)^2 + \beta^2\left(\frac{N_{\mathrm{FLAIR}}}{S_{\mathrm{FLAIR}}}\right)^2, \tag{5}$$

where N_{SyFLAIR3}, N_{T2WI}, and N_{FLAIR} represent the noise for SyFLAIR^3, T2WI, and FLAIR image, respectively. Under the assumption that the noise for the T2WI and FLAIR image is changed under the conditions generated using synthetic MRI, we can derive the following equation:

$$N_{\mathrm{SyFLAIR3}} = S_{\mathrm{SyFLAIR3}} \cdot \sqrt{\frac{\alpha^2 \cdot N_{\mathrm{T2WI}}^2}{S_{\mathrm{T2WI}}^2} + \frac{\beta^2 \cdot N_{\mathrm{FLAIR}}^2}{S_{\mathrm{FLAIR}}^2}}. \tag{6}$$

Moreover, the CSF ratio for SyFLAIR^3 was calculated as an index of the effect of suppression of the CSF signal for each TE combination. The CSF ratio was calculated as follows:

$$\mathrm{CSF\,ratio} = \frac{S_{\mathrm{CSF}}}{S_{\mathrm{GM}}}, \tag{7}$$

where S_{CSF} and S_{GM} represent the signal intensity of the CSF and GM for SyFLAIR^3, respectively. Using these equations, the CNR and CSF ratio for SyFLAIR^3 were calculated for all TE combinations of the T2WI and FLAIR image.

2.3 In vivo study

2.3.1 Imaging protocol and generation of synthetic images

The study was approved by our Institutional Review Board. Ten healthy volunteers (mean age 44.1 years; age range 23–61 years) were enrolled. Written informed consent was obtained from all the participants. The in vivo study was performed using a 3.0-T MRI system (Discovery MR750; GE Healthcare, Waukesha, WI, USA) with a 32-channel phased-array head coil.

To validate the optimal combination of TE values for the T2WI and FLAIR image, images were acquired from participants using a synthetic MRI sequence. Synthetic MRI was performed using MRI compilation (MAGiC) based on the QRAPMASTER pulse sequence [13], which is a two-dimensional, multi-slice, multi-echo, multi-saturation delay saturation-recovery fast spin echo acquisition sequence for images at two TE combinations and four saturation delay time combinations. Imaging parameters were as follows: field-of-view (FOV) = 240 × 240 mm^2; TR = 4000 ms; TE = 21.3 and 85.2 ms; slice thickness = 4 mm; slice gap = 1 mm; number of slices = 24; echo train length = 12; bandwidth = ± 22.7 kHz; number of excitations (NEX) = 1; array spatial sensitivity encoding technique (ASSET) factor = 2; matrix size = 320 × 256; and imaging time = 6 min 8 s.

After acquisition of the image data, the T_1 value, T_2 value, and PD were automatically quantified using the MRI console computer. The fitting algorithm for quantification was performed based on a report by Warntjes et al. [13]. Using the quantified data, synthetic T2WI and FLAIR images were generated at 15,000-ms TR and TE of 20–140-ms range with a 20-ms interval. The TI of the FLAIR images was set to 3000 ms. Parameters for synthetic DIR imaging were as follows: TR = 15,000 ms; TE = 100 ms; first TI = 3750 ms; and second TI = 470 ms.

2.3.2 Production and evaluation of SyFLAIR^3

SyFLAIR^3 was reconstructed from the T2WI and FLAIR image at all combinations of TE using MATLAB 2017a (MathWorks, Natick, MA, USA). To evaluate the image quality of SyFLAIR^3, the signal intensity of the frontal WM, GM in the superior frontal gyrus, CSF in the frontal horn of the lateral ventricle, and WM in the central semiovale for the T2WI, FLAIR image, DIR image, and SyFLAIR^3 was measured using ImageJ 1.5 software

(National Institutes of Health; Bethesda, MD, USA). The WML was assumed as the region in which the T_2 value was prolonged by 15% compared with that of the WM at the level of the basal ganglia, based on the T_2 values of the MS lesions reported through numerical simulation [18]. These regions were located around the central semiovale and confirmed using the T_2 values obtained through MAGiC. In all volunteers, the ROI in the WM was set to 122.6 mm^2. The ROI in the other tissues was changed according to the individuals' tissue morphology. The average ROI was 32.8, 70.4, and 286.0 mm^2 for the GM, CSF, and WML.

Subsequently, the CNR for the T2WI, FLAIR image, DIR image, and SyFLAIR^3 was measured using the following equation:

$$\mathrm{CNR} = \frac{S_{\mathrm{WML}} - S_{\mathrm{WM}}}{\mathrm{SD}_{\mathrm{WM}}}, \tag{8}$$

where S_{WML} and S_{WM} represent the signal intensity of the WML and WM for each image, respectively. $\mathrm{SD}_{\mathrm{WM}}$ represents the standard deviation of the signal intensity of the WM for each image. The CSF ratio for the FLAIR image and SyFLAIR^3 was measured using Eq. 7.

Finally, to determine the optimal combination of T2WI and FLAIR image for SyFLAIR^3, we evaluated the CNR and CSF ratio for SyFLAIR^3 for all TE combinations of the T2WI and FLAIR image acquired in the in vivo study. The optimal TE for the T2WI and FLAIR image was defined as the TE at the maximum CNR for SyFLAIR^3 among TEs at which the CSF ratio for SyFLAIR^3 is lower than that for the FLAIR image at any TE.

2.3.3 Statistical analysis

Nonparametric Wilcoxon matched-pairs rank test was used to compare the CSF ratio between the FLAIR image and SyFLAIR^3. Friedman test was performed to compare the CNR between the FLAIR image, DIR image, and SyFLAIR^3; post hoc tests were performed using Dunn's multiple comparisons test. $P < 0.05$ was considered significant. All statistical analyses were performed using Prism 6.0 (GraphPad Software, La Jolla, CA, USA).

3 Results

3.1 Numerical simulations

Figure 1 shows the CNR and CSF ratio obtained through numerical simulation. The CNR for SyFLAIR^3 was increased at prolonged TE of both the T2WI and FLAIR image; conversely, it was decreased at shortened TE of either the T2WI or FLAIR image. The CSF ratio for SyFLAIR^3 was increased at prolonged TE of both the T2WI and FLAIR image, and was decreased at shortened TE of either the T2WI or FLAIR image.

3.2 In vivo study

The CNR and CSF ratio for the T2WI and FLAIR image acquired from each participant of the in vivo study is shown in Fig. 2. The CNR for the T2WI and FLAIR image increased with prolonging of TE and plateaued at approximately 60 ms; the CNR showed similar value for each TE. The CSF ratio for the T2WI and FLAIR image decreased with shortening of TE. The CNR and CSF ratio

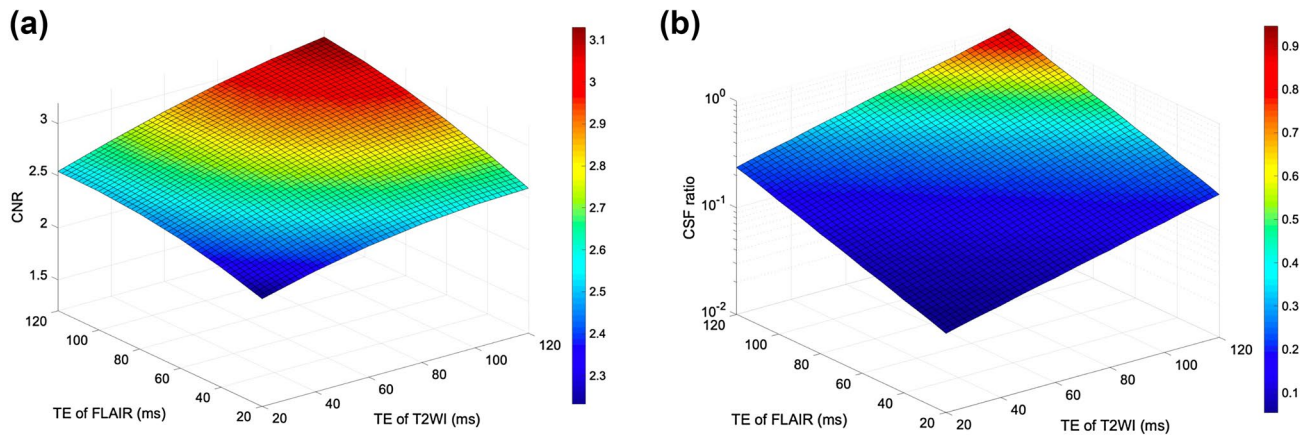

Fig. 1 Results of the numerical simulation for the CNR for SyFLAIR^3 versus the TEs of the T2WI and FLAIR image. **a** The CSF ratio for SyFLAIR^3 versus the TEs of the T2WI and FLAIR image. **b** The CNR and CSF ratio show increases with longer TEs for both the T2WI and FLAIR image

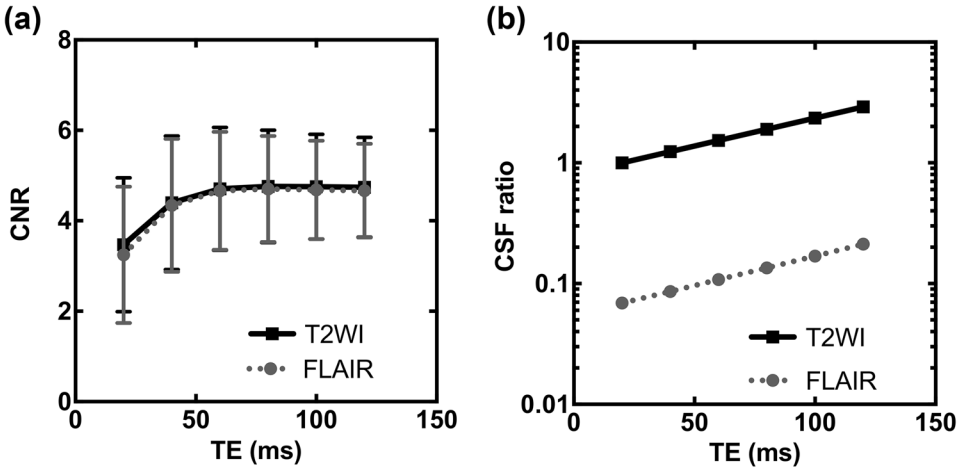

Fig. 2 The CNR (**a**) and CSF ratio (**b**) for the T2WI and FLAIR image acquired in the in vivo study. The CNRs for the T2WI and FLAIR image are increased at prolonged TEs and plateau at approximately 60 ms. The CNRs for both the T2WI and FLAIR image demonstrate comparable values at each TE. The CSF ratios for the T2WI and FLAIR image are decreased at shorter TEs

for SyFLAIR[3] produced through in vivo imaging data are shown in Fig. 3.

The CNR for SyFLAIR[3] was increased with a combination of longer TEs for both the T2WI and FLAIR image as well as that through numerical simulation. The CSF ratio for SyFLAIR[3] calculated using different TE combinations for both the T2WI and FLAIR image acquired through the in vivo study showed similar tendency to those through the numerical simulation.

To determine the optimal TE combination of the T2WI and FLAIR image for SyFLAIR[3], we considered that the CSF ratio for SyFLAIR[3] should be less than or equal to that for the FLAIR image at any TE; the combinations of TEs that meet this condition are located below the dotted line shown in Fig. 3b. Among the combinations that matched this condition, the maximum CNR value was obtained by the following five combinations of TEs for the T2WI and FLAIR images: (20 ms, 100 ms), (40 ms, 80 ms), (60 ms, 60 ms), (80 ms, 40 ms), and (100 ms, 20 ms), as shown in Fig. 3a. These results indicated that the optimal TE combination for SyFLAIR[3] reconstruction was 60 ms for both the T2WI and FLAIR image according to the simplest combination.

The CNR (average ± standard deviation) for the FLAIR image with a 100-ms TE (which was the largest CNR for all values of TE), DIR image, and SyFLAIR[3] with the optimal combination of T2WI and FLAIR image was 4.69 ± 1.08, 3.20 ± 1.74, and 5.52 ± 1.69, respectively (Fig. 4a). The CNR for optimized SyFLAIR[3] was significantly higher than those for the FLAIR and DIR images. The CSF ratio (average ± standard deviation) for the FLAIR image with a 20-ms TE and SyFLAIR[3] with the optimal combination of the T2WI was 0.069 ± 0.0019 and 0.059 ± 0.0071, respectively (Fig. 4b). The CSF ratio was significantly lower in the optimized SyFLAIR[3] versus the that in the FLAIR image with a 20-ms TE which was the smallest CSF ratio for all values of TE. Representative

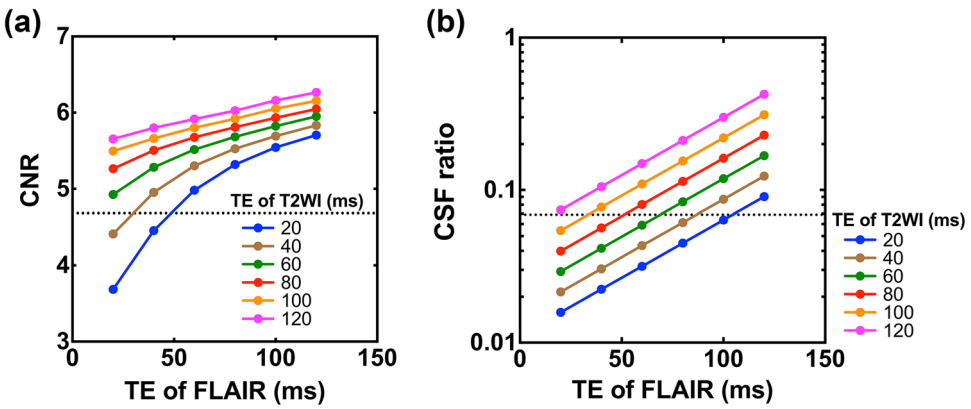

Fig. 3 The CNR for SyFLAIR[3] generated by combining TEs from the T2WI and FLAIR image. The dotted line shows the CNR for FLAIR images at 100-ms TE, which is the maximum CNR for all TEs of the FLAIR image (**a**). The CSF ratio for SyFLAIR[3] generated by combining TEs from the T2WI and FLAIR image. The dotted line shows the CSF ratio for the FLAIR image at 20-ms TE, which is the minimum CSF ratio for all TEs of the FLAIR image (**b**). The CNR for SyFLAIR[3] is increased with a combination of longer TEs for the T2WI and FLAIR image. The CSF ratio for SyFLAIR[3] is decreased with a combination of short TEs for the T2WI and FLAIR image

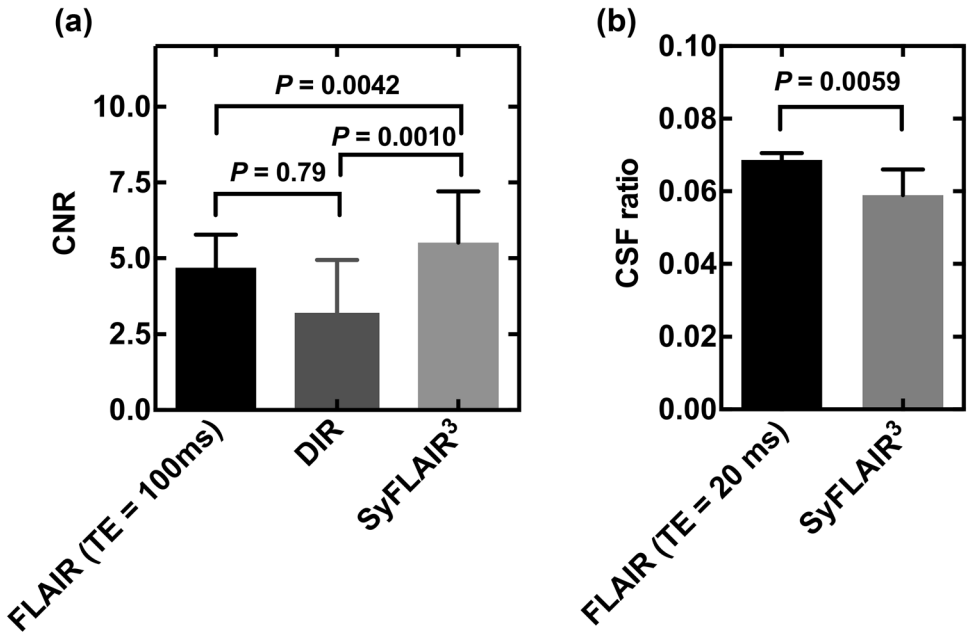

Fig. 4 The CNRs (**a**) and CSF ratios (**b**) from the in vivo study for the FLAIR image, DIR image, and SyFLAIR[3]. The CNRs are significantly higher for the optimized SyFLAIR[3] than for the FLAIR images (TE = 100 ms) and DIR images (TE = 100 ms). The CSF ratios are significantly lower for the optimized SyFLAIR[3] than for the FLAIR images (TE = 20 ms)

images for FLAIR, DIR, and SyFLAIR[3] at the level of the basal ganglia and central semiovale are shown in Fig. 5. The optimized SyFLAIR[3] at the level of the basal ganglia indicated that the CSF signal in the lateral ventricle was suppressed to a comparable degree as that on the FLAIR and DIR images (Fig. 5a–c). Moreover, the optimized SyFLAIR[3] at the level of the central semiovale indicated that the contrast within the WM region was higher than that on the FLAIR and DIR images (Fig. 5d–f).

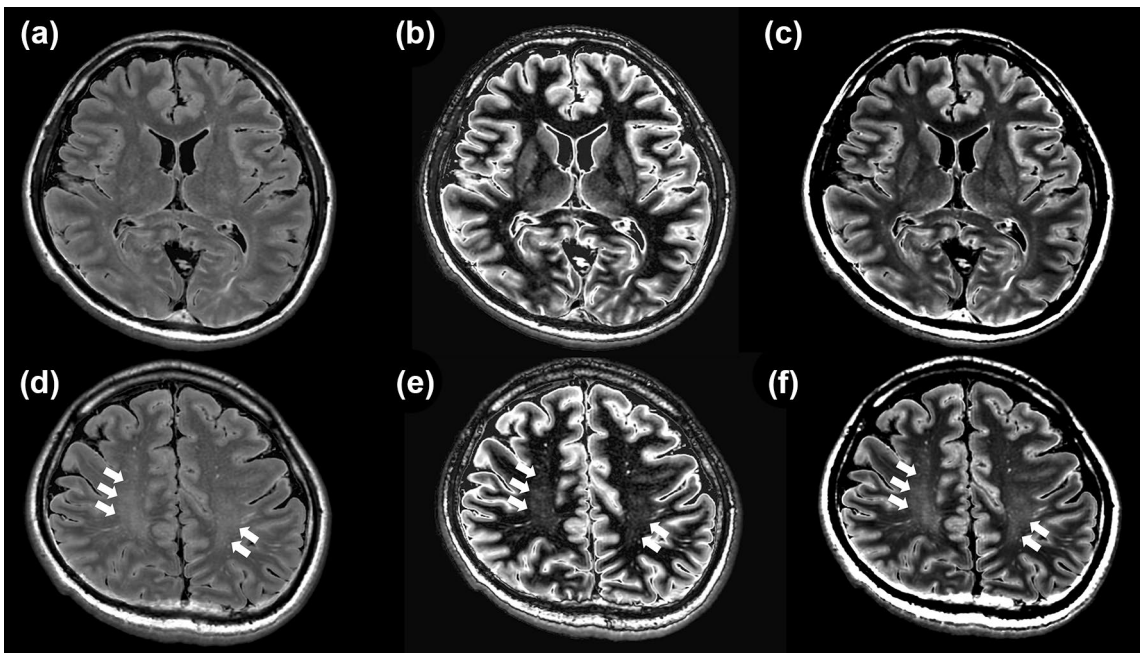

Fig. 5 A comparison of representative FLAIR images (TE = 100 ms) (**a, d**), DIR images (**b, e**), and optimized SyFLAIR[3] (**c, f**) calculated at 60-ms TE for both the T2WI and FLAIR image at the level of the basal ganglia and central semiovale. The optimized SyFLAIR[3] at the level of the basal ganglia shows that the CSF signal in the lateral ventricle is suppressed to a comparable degree as that on the FLAIR and DIR images (**a–c**). Moreover, the optimized SyFLAIR[3] at the level of the central semiovale shows that the contrast within the WM region is greater than that on the FLAIR and DIR images (**d–f**)

4 Discussion

We demonstrated that the SyFLAIR^3 post-processing technique could be applied to synthetic MRI and improved the CNR of the WM region under optimal reconstruction settings.

The results of the numerical simulation indicated that when the previously reported FLAIR$_3$ technique was applied to synthetic MRI, the CNR for SyFLAIR^3 varied depending on the combination of TEs for the T2WI and FLAIR image. To attain a higher CNR for SyFLAIR^3, a combination of longer TEs for both the T2WI and FLAIR image was needed. In contrast, the CSF ratio increased at longer TEs for both the T2WI and FLAIR image. Therefore, to effectively suppress the CSF signal, a shorter TE is preferable for the T2WI and FLAIR image. To satisfy these two conflicting requirements and apply FLAIR$_3$ to synthetic MRI, it is necessary to determine the optimal TE combination for the T2WI and FLAIR image based on both the CNR and CSF ratio.

In the in vivo study, the CNR for the T2WI and FLAIR image reconstructed for each TE using synthetic MRI was higher at longer TEs. To apply these images to SyFLAIR^3 and obtain a higher CNR, images at longer TEs should be used. In contrast, the CSF ratio for the T2WI and FLAIR image showed a linear increase on the log scale with increasing value of TE, which indicates that a combination of short TEs for both the T2WI and FLAIR image was effective in suppressing the CSF signal for SyFLAIR^3, corroborating the results through numerical simulation. When the CSF ratio for SyFLAIR^3 was less than that for the FLAIR image with a 20-ms TE (Fig. 4b), the five combinations of TEs showed maximal CNR. Among these combinations, the combination of 60-ms TE for both the T2WI and FLAIR image is the simplest one for maximizing the CNR. This result is useful for application of SyFLAIR^3 in the clinical setting.

The optimized SyFLAIR^3 significantly improved the CNR of the WM compared with those on the T2WI and FLAIR image reconstructed using synthetic MRI. Furthermore, the optimized CSF ratio for SyFLAIR^3 was significantly decreased compared with that for the FLAIR image with a 20-ms TE. Our results are consistent with those reported for 3D T2WI and 3D FLAIR [18]. Thus, the image-processing technique of FLAIR$_3$ could be applied to synthetic MRI, and SyFLAIR^3 could enable the detection of WMLs such as the MS plaque.

Gabr et al. described the image-processing technique of FLAIR$_3$ involving pre-acquired images through 3D T2WI and 3D FLAIR [18]. Since these images are acquired using a prolonged scanning time, displacement within each image may occur due to the patients' motion. Therefore, before FLAIR$_3$ processing, a pre-processing step such as affine transformation is needed to avoid artifacts due to misalignment.

In contrast, synthetic MRI can acquire images arbitrarily and simultaneously, such as the T2WI and FLAIR image through computed quantitative values. Consequently, corrections are not required to process SyFLAIR^3 for positional misalignment between the T2WI and FLAIR image. In addition, synthetic MRI has the advantage of ability to generate T2WI and FLAIR images at any TE, which is necessary for producing SyFLAIR^3 without additional imaging. Therefore, once proper conditions for calculating SyFLAIR^3 are determined, SyFLAIR^3 is automatically generated with ease as a post-processing step. In this study, the production of SyFLAIR3 was performed offline; nevertheless, it may be possible to incorporate these steps into the calculation of SyFLAIR^3 as an easy-to-use option for synthetic MRI in the clinical setting. Reports indicated that FLAIR and DIR images generated through synthetic MRI improved the CNR of the WM and WMLs [6, 15]. Based on the improved CNR for SyFLAIR^3 compared with those for the FLAIR and DIR images, SyFLAIR^3 has potential for use to detect MS lesions more easily.

This study has several limitations. First, although the results obtained through numerical simulation and in vivo study were similar, they were not matched perfectly, which may be due to the insufficient definition of noise in the numerical simulation. Second, we did not evaluate patients with WMLs, such as MS lesions. Future studies to verify improvement in the CNR of WMLs in clinical cases are necessary. Third, we did not optimize the coefficients of the exponent used to produce SyFLAIR^3. Regarding the multiplication coefficients, although verified values from a previous report were used, further optimization may yield greater improvement in the CNR. Finally, DIR images were generated using the manufacturer's default TI settings. Hagiwara et al. estimated the optimal second TI for each patient by measuring the T_2 values of the WM and CSF to generate DIR images using synthetic MRI [15]. Although the DIR images were generated using the optimal second TI in order to increase the contrast between the WM and WML, adjusting the parameters for each patient is not considered as standard procedure in clinical practice. In routine general clinical examinations, a fixed second TI is used. Moreover, in our study, the T_2 values of the WM were almost the same in all participants; therefore, we used 470 ms as the second TI in agreement with the previous report [16].

In conclusion, SyFLAIR^3 produced using synthetic MRI improved the CNR of the WM region compared with that for the FLAIR and DIR images. Although clinical studies are needed to evaluate the clinical utility of SyFLAIR^3, it could be useful to detect WMLs such as the MS plaque.

Acknowledgements The authors would like to thank Yoshiyuki Ishimori, PhD, for his useful suggestions. This study was supported in part by Grant-in-Aid for Scientic Research (C) from Japan Society for the Promotion of Science (Grant no. 15K09916).

Compliance with ethical standards

Conflict of interest The authors declare no conflict of interest.

Ethical approval Statements of human rights: All procedures performed in studies involving human participants were in accordance with the ethical standards of our Institutional Review Board (IRB) and 1964 Helsinki Declaration and its later amendments or comparable ethical standards. Statements of animal rights: This article does not contain any studies performed on animals.

Informed consent Informed consent was obtained from each participant included in this study.

References

1. Polman CH, Reingold SC, Banwell B, et al. Diagnostic criteria for multiple sclerosis: 2010 revisions to the McDonald criteria. Ann Neurol. 2011;69:292–302.
2. Simon JH, Li D, Traboulsee A, et al. Standardized MR imaging protocol for multiple sclerosis: consortium of MS centers consensus guidelines. Am J Neuroradiol. 2006;27:455–61.
3. Bachmann R, Reilmann R, Schwindt W, et al. FLAIR imaging for multiple sclerosis: a comparative MR study at 1.5 and 3.0 T. Eur Radiol. 2006;16:915–21.
4. Stevenson VL, Parker GJ, Barker GJ, et al. Variations in T1 and T2 relaxation times of normal appearing white matter and lesions in multiple sclerosis. J Neuro Sci. 2000;178:81–7.
5. Miller DH, Johnson G, Tofts PS, et al. Precise relaxation time measurements of normal-appearing white matter in inflammatory central nervous system disease. Magn Reson Med. 1989;11:331–6.
6. Armspach JP, Gounot D, Rumbach L, et al. In vivo determination of multiexponential T2 relaxation in the brain of patients with multiple sclerosis. Magn Reson Imaging. 1991;9:107–13.
7. Hagiwara A, Hori M, Yokoyama K, et al. Utility of a multiparametric quantitative MRI model that assesses myelin and edema for evaluating plaques, periplaque white matter, and normal-appearing white matter in patients with multiple sclerosis: a feasibility study. Am J Neuroradiol. 2017;38:237–42.
8. Granberg T, Uppman M, Hashim F, et al. Clinical feasibility of synthetic MRI in multiple sclerosis: a diagnostic and volumetric validation study. Am J Neuroradiol. 2016;37:1023–9.
9. Blystad I, Warntjes JB, Smedby O, et al. Synthetic MRI of the brain in a clinical setting. Acta Radiol. 2012;53:1158–63.
10. Wattjes MP, Lutterbey GG, Gieseke J, et al. Double inversion recovery brain imaging at 3 T: diagnostic value in the detection of multiple sclerosis lesions. Am J Neuroradiol. 2007;28:54–9.
11. Geurts JJ, Pouwels PJ, Uitdehaag BM, et al. Intracortical lesions in multiple sclerosis: improved detection with 3D double inversion-recovery MR imaging. Radiology. 2005;236:254–60.
12. Redpath W, Smith W. Use of a double inversion recovery pulse sequence to image selectively grey or white brain matter. Br J Radiol. 1994;67:1258–63.
13. Warntjes JB, Leinhard OD, West J, et al. Rapid magnetic resonance quantification on the brain: optimization for clinical usage. Magn Reson Med. 2008;60:320–9.
14. Hagiwara A, Warntjes M, Hori M, et al. SyMRI of the brain: rapid quantification of relaxation rates and proton density, with synthetic MRI, automatic brain segmentation, and myelin measurement. Investig Radiol. 2017;52:647.
15. Hagiwara A, Hori M, Yokoyama K, et al. Synthetic MRI in the detection of multiple sclerosis plaques. Am J Neuroradiol. 2016;38:257–63.
16. Wiggermann V, Hernández-Torres E, Traboulsee A, et al. FLAIR^2: a combination of FLAIR and T2 for improved MS lesion detection. Am J Neuroradiol. 2016;37:259–65.
17. Sati P, George IC, Shea CD, et al. FLAIR*: a combined MR contrast technique for visualizing white matter lesions and parenchymal veins. Radiology. 2012;265:926–32.
18. Gabr RE, Hasan KM, Haque ME, et al. Optimal combination of FLAIR and T2-weighted MRI for improved lesion contrast in multiple sclerosis. J Magn Reson. 2016;44:1293–300.